

# Pion transverse charge density from $e^+e^-$ annihilation data and logarithmic dispersion relations

Enrique Ruiz Arriola<sup>a,b</sup>, Pablo Sanchez-Puertas<sup>a</sup>, Christian Weiss<sup>c</sup>

<sup>a</sup>*Departamento de Física Atómica, Molecular y Nuclear, Universidad de Granada, E-18071, Granada, Spain*

<sup>b</sup>*Instituto Carlos I de Física Teórica y Computacional, Universidad de Granada, E-18071, Granada, Spain*

<sup>c</sup>*Theory Center, Jefferson Lab, Newport News, VA 23606, USA*

## Abstract

The transverse charge density of the pion is extracted from a dispersive analysis of the  $e^+e^- \rightarrow \pi^+\pi^-$  exclusive annihilation data. A logarithmic dispersion relation is used to compute the unknown phase of the timelike pion form factor from the modulus obtained from the annihilation cross section. The method is model-independent and permits quantitative uncertainty estimates. The density is obtained with few-percent accuracy down to  $b \sim 0.1$  fm; at smaller distances it depends qualitatively on the assumed high-energy behavior of the timelike form factor. Implications for pion structure and the relevance of pQCD asymptotics are discussed.

**Keywords:** Pion form factor, dispersion relations, annihilation experiments, quantum chromodynamics

## 1. Introduction

The internal structure of the pion plays a central role in quantum chromodynamics (QCD) and its application to hadronic systems. The pion is the Goldstone boson associated with the spontaneous breaking of chiral symmetry, and its structure is governed by the non-perturbative interactions causing this effect. The charged pion form factor (FF) and the neutral pion transition FF at momentum transfers  $Q^2 \gg 1$  GeV<sup>2</sup> are the simplest hadron FFs that can be analyzed using QCD factorization [1–6], and their study is an important testing ground for perturbative QCD (pQCD) interactions [7].

The transverse charge density is a powerful tool for quantifying pion structure in QCD. It is defined as the two-dimensional Fourier transform of the pion FF  $F_\pi^Q(q^2)$  at spacelike momentum transfers  $q^2 = -Q^2 < 0$  and describes the distribution of charge in transverse position at fixed light-front time [8–11]. It provides a concept of spatial density appropriate for the relativistic system and corresponds to a genuine quantum-mechanical expectation value of the electromagnetic current in the localized pion state. In the partonic picture, the transverse density represents a projection of the generalized parton distributions (GPDs) in the pion and provides information on the distribution of quarks/antiquarks in the system [12–14]. In the hadronic picture, the transverse density is analyzed using methods based on analyticity and unitarity and expresses the dynamics of hadronic exchange mechanisms. As such the transverse density allows one to connect partonic structure with hadronic dynamics and offers unique insight into hadron structure.

The pion FF at timelike momentum transfers  $q^2 = s$  is measured in exclusive annihilation experiments  $e^+e^- \rightarrow \pi^+\pi^-$  [15]. Through the dispersion relations for the complex function  $F_\pi^Q(q^2)$ , these data can be used to extract the spacelike FF and the transverse density [16]. The standard dispersion relation re-

quires knowledge of the imaginary part  $\text{Im} F_\pi^Q(s)$  at  $s > 4M_\pi^2$ , while the experiments only provide the modulus  $|F_\pi^Q(s)|^2$ . This necessitates the use of model-dependent methods (e.g. fits by a superposition of resonances [17]) to reconstruct the phase of the FF. An alternative approach is the use of logarithmic (or phase-modulus) dispersion relations, which reconstruct the phase of the FF from the  $s$ -dependence of the measured  $|F_\pi^Q(s)|^2$ , provided the FF has no complex zeros [18, 19]. The method is unique to the pion FF, for which  $|F_\pi^Q(s)|^2$  can be measured starting from the threshold at  $s = 4M_\pi^2$ , and becomes practical thanks to the high precision of the annihilation data. It offers several advantages over the conventional dispersive analysis: it avoids model dependence, works directly with experimental data, and permits quantitative uncertainty estimates. An extraction of the phase of the pion FF using logarithmic dispersion relations was performed recently in Ref. [20] (see also [21]).

In this work we analyze the pion transverse charge density using logarithmic dispersion relations and the results of Ref. [20]. We extract the empirical density over a wide range of distances and compare its behavior with theoretical expectations based on pQCD, vector resonances and unitarity, and chiral dynamics. Our approach offers several new aspects: (i) It represents a unique case of “transverse imaging” based directly on experimental data. (ii) It permits simple and efficient statistical uncertainty quantification of the transverse density, avoiding issues with Fourier transform of spacelike FF data. (iii) It constrains the density at distances  $\gtrsim 0.1$  fm with smaller fit uncertainties than other methods. (iv) It provides an estimate of the dominant theoretical uncertainty based on QCD arguments.

## 2. Transverse density and dispersive representation

The transverse charge density is defined as the 2-dimensional Fourier transform (radial Fourier–Bessel transform) of the

spacelike pion FF,

$$\rho_\pi(b) = \int_0^\infty \frac{dQ}{2\pi} Q J_0(Qb) F_\pi^Q(-Q^2). \quad (1)$$

It describes the distribution of charge with respect to the distance  $b$  from the transverse center of momentum, with  $\int d^2b \rho_\pi(b) = 1$ ; for its interpretation and connection with GPDs, see Refs. [9–11]. Using the analytic properties one can express the density in terms of the FF in the timelike region. The pion FF satisfies an unsubtracted dispersion relation,

$$F_\pi^Q(-Q^2) = \int_{s_0}^\infty ds \frac{\text{Im} F_\pi^Q(s)}{\pi(s + Q^2 - i0)}, \quad (2)$$

where  $\text{Im} F_\pi^Q(s)$  is the imaginary part on the cut at  $s > s_0 \equiv 4M_\pi^2$ . Substituting this representation into Eq. (1) and performing the Fourier integral one obtains [22]

$$\rho_\pi(b) = \int_{s_0}^\infty \frac{ds}{2\pi^2} K_0(\sqrt{sb}) \text{Im} F_\pi^Q(s), \quad (3)$$

where  $K_0$  is the modified Bessel function. This dispersive representation of the density has several useful properties: (i) The kernel decays exponentially at large arguments,  $K_0(x) \sim \sqrt{\pi/2} \exp(-x)/\sqrt{x}$  for  $x \gg 1$ , so that the dispersion integral converges exponentially at large energies, to be compared with the oscillating behavior of  $J_0$  in Eq. (1). (ii) The range of  $\sqrt{s}$  covered in the integral is determined by the inverse distance,  $1/b$ , and the density can be regarded as an ‘‘exponential filter’’ sampling the timelike FF.<sup>1</sup> (iii) The kernel is positive,  $K_0 > 0$ , simplifying the uncertainty propagation from the pion FF into the density. (iv) The dispersive representation embodies the analytic properties of the FF and produces densities with the correct asymptotic behavior at  $b \rightarrow \infty$ , enabling mathematically stable computation of densities at large distances [25].

### 3. Basic properties and asymptotic behavior

Several properties of the transverse density can be derived directly from the dispersive representation Eq. (3) and will be of relevance in what follows.

*Large distances and threshold behavior.* At distances  $b \gg M_\pi^{-1}$  the dispersion integral is dominated by energies near the threshold,  $s = s_0 + \text{few } M_\pi^2$ . Below the  $4\pi$  threshold at  $s = 16M_\pi^2$ , the phase of the pion FF is determined by elastic unitarity (Watson’s theorem),

$$F_\pi^Q(s) = |F_\pi^Q(s)| e^{i\delta_1^1(s)}, \quad \text{Im} F_\pi^Q(s) = |F_\pi^Q(s)| \sin \delta_1^1(s), \quad (4)$$

where  $\delta_1^1$  is the phase shift of  $\pi\pi$  scattering in the  $I = J = 1$  isospin and angular momentum channel. In terms of the partial-wave amplitude (in the convention of Ref. [26])

$$f_1^1(s) \equiv e^{i\delta_1^1(s)} \sin \delta_1^1(s) \sqrt{s}/(2k_\pi), \quad (5)$$

where  $k_\pi \equiv \sqrt{s/4 - M_\pi^2}$  is the  $\pi\pi$  CM momentum, the threshold expansion is given by

$$\text{Re} f_1^1(s) = \frac{\sqrt{s}}{4k_\pi} \sin(2\delta_1^1(s)) = 2M_\pi k_\pi^2 (a_1^1 + b_1^1 k_\pi^2 + \dots), \quad (6)$$

where  $a_1^1$  and  $b_1^1$  are the slope parameters. For the imaginary part this implies

$$\text{Im} F_\pi^Q(s) = |F_\pi^Q(4M_\pi^2)| a_1^1 k_\pi^3 + \mathcal{O}(k_\pi^5). \quad (7)$$

The asymptotic behavior of the density is then obtained from Eq. (3) as

$$\rho_\pi(b) \sim \frac{3M_\pi^2 |F_\pi^Q(4M_\pi^2)| a_1^1}{2\pi b^3} e^{-2M_\pi b} \quad (b \gg M_\pi^{-1}). \quad (8)$$

Chiral perturbation theory provides approximate predictions for the threshold parameters. At LO accuracy [26]

$$a_1^1 = 2/(96\pi F_\pi^2 M_\pi) + \dots, \quad |F_\pi^Q(4M_\pi^2)| = 1 + \dots, \quad (9)$$

where  $F_\pi = 92$  MeV is the pion decay constant, and the asymptotic behavior Eq. (8) becomes

$$\rho_\pi(b) \sim \frac{3M_\pi}{96\pi^2 F_\pi^2 b^3} e^{-2M_\pi b} \quad (b \gg M_\pi^{-1}). \quad (10)$$

At what values of  $b$  the asymptotic behavior Eq. (8) becomes relevant, and how accurately the absolute prediction Eq. (10) describes the asymptotic density, are questions that can be answered by the empirical results.

*Intermediate distances and vector meson dominance.* The inelasticity in  $\pi\pi$  scattering remains small up to the  $K\bar{K}$  threshold [27, 28], and the elastic unitarity approximation Eq. (4) for the timelike FF can be used up to  $s_1 = 4M_K^2 \approx 1 \text{ GeV}^2$  [15]. For the density this implies

$$\rho_\pi(b) \approx \int_{s_0}^{s_1} \frac{ds}{2\pi^2} K_0(\sqrt{sb}) |F_\pi^Q(s)| \sin \delta_1^1(s) + \mathcal{O}(e^{-\sqrt{s_1}b}). \quad (11)$$

In this region the phase shift is dominated by the  $\rho$  resonance, and the density decays exponentially with the  $\rho$  meson mass. A zero-width resonance, with a coupling chosen such that  $F_\pi^Q(0) = 1$ , corresponds to  $\text{Im} F_\pi^Q(s) = \pi M_\rho^2 \delta(s - M_\rho^2)$  in Eq. (2) and provides an approximation to the density in Eq. (3) as

$$\rho_\pi(b) = (M_\rho^2/2\pi) K_0(M_\rho b). \quad (12)$$

This dynamics governs the behavior of density at intermediate distances  $b \sim 1/M_\rho$  and can be seen in the empirical results.

*Small distances and pQCD.* The asymptotic behavior of the density at  $b \rightarrow 0$  can be derived from Eq. (3) using the pQCD approximation for the timelike pion FF. The asymptotic behavior of the spacelike pion FF is given by the well-known expression resulting from the  $\mathcal{O}(\alpha_s)$  hard scattering process and the asymptotic pion distribution amplitudes [1–6],

$$F_\pi^Q(-Q^2) = \frac{16\pi F_\pi^2 \alpha_s(Q^2)}{Q^2} [1 + \mathcal{O}(\alpha_s)], \quad (13)$$

<sup>1</sup>This property is similar to the so-called Laplace sum rules for Euclidean correlation functions [23, 24].

where the running coupling  $\alpha_s$  is taken at the scale  $Q^2$ . At LO accuracy the coupling is given by  $\alpha_s(Q^2) = 4\pi/[\beta_0 \log(Q^2/\Lambda_{\text{QCD}}^2)]$ , where  $\beta_0 = (11N_c - 2N_f)/3$  and  $\Lambda_{\text{QCD}}$  is the QCD scale parameter. Analytic continuation to timelike momenta is performed by setting  $Q^2 = -s - i0$  and continuing from  $s < 0$  to  $s > 0$ , resulting in

$$\alpha_s \rightarrow \frac{4\pi}{\beta_0[\ln(s/\Lambda_{\text{QCD}}^2) - i\pi]}. \quad (14)$$

The imaginary part of the pion FF in LO is thus given by

$$\text{Im } F_\pi^Q(s) = -\frac{64\pi^3 F_\pi^2}{\beta_0 s [\log^2(s/\Lambda_{\text{QCD}}^2) + \pi^2]}. \quad (15)$$

The negative sign unambiguously follows from the analytic continuation. Because at low and intermediate energies  $\text{Im } F_\pi^Q(s) > 0$ , see Eqs. (7) and (9), Eq. (15) implies that  $\text{Im } F_\pi^Q(s)$  must change sign as a function of  $s$ . This is indeed seen in the empirical timelike FF (see Fig. 1) [20].

The imaginary part of the pion timelike FF obeys the sum rules [29, 30]

$$\frac{1}{\pi} \int_{s_0}^{\infty} ds \frac{\text{Im } F_\pi^Q(s)}{s} = 1, \quad (16)$$

$$\frac{1}{\pi} \int_{s_0}^{\infty} ds \text{Im } F_\pi^Q(s) = 0. \quad (17)$$

The first relation follows from the pion charge,  $F_\pi^Q(0) = 1$ . The second relation expresses the absence of a  $1/Q^2$  power term in the asymptotic expansion of the spacelike FF at large  $Q^2$ , as required by pQCD. Note that the large- $s$  behavior of  $\text{Im } F_\pi^Q(s)$  in pQCD, Eq. (15), is such that the integral Eq. (17) converges. The sum rules Eqs. (16) and (17) by themselves imply that  $\text{Im } F_\pi^Q(s)$  must change sign as a function of  $s$ , as observed in the explicit expressions above.

The pQCD prediction for the imaginary part, Eq. (15), combined with the sum rule Eq. (17), implies a certain asymptotic behavior of the density at small distances. Expanding the kernel in Eq. (3),  $K_0(x) = -\log(x) - \log(e^{\gamma_E}/2) + \mathcal{O}[x^2 \log(x)]$  for  $x \ll 1$ , we obtain

$$\rho_\pi(b) = \int_{s_0}^{\infty} \frac{ds}{2\pi^2} \left[ -\log(\sqrt{s}b) - \log(e^{\gamma_E}/2) \right] \text{Im } F_\pi^Q(s). \quad (18)$$

Separating the arguments in the first logarithm, the coefficient of  $-\log b - \log(e^{\gamma_E}/2)$  vanishes due to Eq. (17) (this finding will have important implications later). The asymptotic behavior of  $\rho_\pi(b)$  results from the  $-\log \sqrt{s}$  term and is computed by restricting the integral to values  $\sqrt{s}b \ll 1$ , giving

$$\rho_\pi(b) \sim \frac{16\pi F_\pi^2}{\beta_0} [\log \log(1/b\Lambda_{\text{QCD}}) + c] + \mathcal{O}[1/\log(b)], \quad (19)$$

where  $c$  is a constant that governs the numerical approach to the double logarithmic asymptotic behavior; the choice of  $\Lambda_{\text{QCD}}$  as mass scale in the double logarithm is arbitrary and determines the value of the constant. The asymptotic behavior Eq. (19)

agrees with the one derived from the spacelike FF in Ref. [31]. It is derived from pQCD and not expected to be applicable at practically achievable energies, as seen in the empirical results; see Refs. [32, 33] for further discussion. In particular, Eq. (19) relies on the asymptotic sum rule Eq. (17); any nonzero value of the integral would produce a  $\log(1/b)$  asymptotic behavior, which would overrule that of Eq. (19).

#### 4. Imaginary part from logarithmic dispersion relation

To evaluate the density in the dispersive representation Eq.(3) one needs the imaginary part of the pion FF over a broad range of energies. Exclusive annihilation experiments  $e^+e^- \rightarrow \pi^+\pi^-$  measure the squared modulus  $|F_\pi^Q(s)|^2$  starting from the threshold  $s = s_0$ . The phase of the FF can be reconstructed from the  $s$ -dependence of the modulus using logarithmic dispersion relations. To derive them one sets  $F_\pi^Q(s) = |F_\pi^Q(s)|e^{i\delta(s)}$ , assumes that  $F_\pi^Q(s)$  has no zeroes in the complex plane, and writes a dispersion relation for the complex function  $\log F_\pi^Q(s)/(s_0 - s)^{n+1/2}$  with  $n = 0, 1, \dots$ , which has the same cut as the original  $F_\pi^Q(s)$ . The dispersion relation for  $n = 1$  is obtained as [20]

$$\delta(s) = \frac{-s(s - s_0)^{3/2}}{2\pi} \text{P} \int_{s_0}^{\infty} ds' \frac{\log |F_\pi^Q(s')/F_\pi^Q(s_0)|^2}{s'(s' - s)(s' - s_0)^{3/2}} - (s/s_0 - 1)^{3/2} \log F_\pi^Q(s_0); \quad (20)$$

it incorporates the condition  $F_\pi^Q(0) = 1$  and implements the correct  $P$ -wave threshold behavior. If the variation of the logarithm is limited,  $\log |F_\pi^Q(s')/F_\pi^Q(s_0)| \sim \text{const}$ , the integrand in Eq. (20) behaves as  $\sim (s')^{-7/2}$  at large  $s'$ , providing rapid convergence. Eq. (20) is therefore well suited for numerical evaluation.

An extraction of the phase of the pion FF using Eq. (20) was performed in Ref. [20]. The analysis used the BaBar data [34] and obtained the phase with controlled uncertainties up to  $s_{\text{max}} = (2.5 \text{ GeV})^2$ ; see Ref. [20] for discussion of the data selection. Various methods were employed to interpolate the data at  $s > (0.6 \text{ GeV})^2$  (Gounaris-Sakurai parametrization [35], linear interpolation) and produced consistent results. Uncertainties were estimated using a MC procedure, fully accounting for correlations without bias. The method enables propagation of the uncertainties into functions derived from the phase, such as the transverse charge density.

Figure 1 shows the imaginary part of the FF obtained from the analysis of Ref. [20]. The inner band represents the statistical uncertainty estimated with a MC procedure; the outer band includes also the interpolation uncertainty. One observes: (i) At  $s \lesssim 1 \text{ GeV}^2$  the imaginary part is dominated by the  $\rho$  resonance, as predicted by elastic unitarity, Eq. (4). (ii) At higher  $s$  the imaginary part exhibits a pattern of resonances with alternating sign, with the  $\rho'$  and  $\rho''$  clearly established and two further peaks suggested. The same pattern was obtained in a resonance-based fit to the timelike FF data [17] and a dispersive analysis of the spacelike data [32] and is well-established in the dispersive approach. (iii) The behavior at large  $s$  appears to be qualitatively consistent with an approach to a negative value as predicted by pQCD; see the LO expression in Eq. (15). The

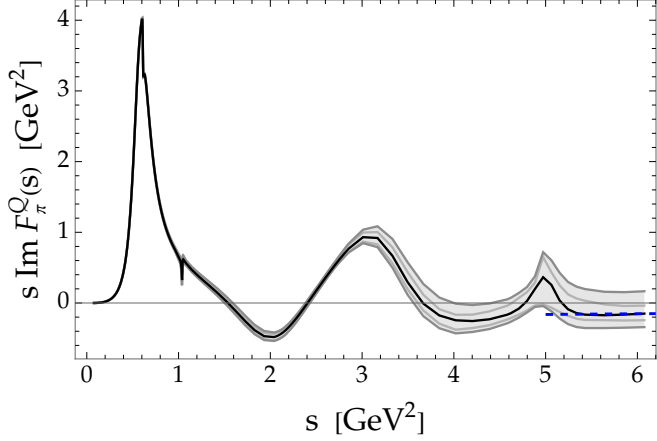


Figure 1: Imaginary part of the pion FF,  $s \text{Im} F_\pi^Q(s)$ , extracted from the logarithmic dispersion relation analysis of Ref. [20]. *Black line*: Central value. *Inner gray band*: Statistical uncertainty. *Outer gray band*: Total uncertainty. *Dashed blue line*: pQCD prediction Eq. (21) (details in text).

dashed blue line shows  $\text{Im} F_\pi^Q(s)$  corresponding to the NNLO prediction for the timelike FF [36, 37]<sup>2</sup>

$$F_\pi^Q(s) = -\frac{16\pi F_\pi^2 \alpha_s}{s} \left( 1 + 6.58 \frac{\alpha_s}{\pi} \left[ 1 + 8.69 \frac{\alpha_s}{\pi} \right] \right), \quad (21)$$

where  $\alpha_s$  is the timelike coupling evaluated with the LO expression Eq. (14) with  $\Lambda_{\text{QCD}} = 250$  MeV; the effect of higher-order corrections to  $\alpha_s$  is negligible compared to the corrections to the FF in Eq. (21). The approach of the empirical FF to the pQCD prediction should be understood on average, as suggested by the Phragmen-Lindelöf theorem for the asymptotic behavior of complex functions with branch cut singularities [18] and the phenomenology of quark-hadron duality. For further discussion of the asymptotic behavior of  $\text{Im} F_\pi^Q(s)$  in pQCD, see Refs. [38, 39].

For the following it will be important to quantify the convergence of the sum rules Eqs. (16) and (17). Integrating the empirical  $\text{Im} F_\pi^Q(s)$  over  $s$  up to  $s_{\text{max}}$  we obtain

$$\frac{1}{\pi} \int_{s_0}^{s_{\text{max}}} ds \frac{\text{Im} F_\pi^Q(s)}{s} \Big|_{\text{Data}} = 1.01(1)_{\text{st}}(-1)_{\text{sys}}, \quad (22)$$

$$\frac{1}{\pi} \int_{s_0}^{s_{\text{max}}} ds \text{Im} F_\pi^Q(s) \Big|_{\text{Data}} = 0.63(2)_{\text{st}}(+7)_{\text{sys}} \text{ GeV}^2. \quad (23)$$

The partial integral Eq. (22) satisfies the charge sum rule Eq. (16) within uncertainties. The partial integral Eq. (23) has a significant non-zero value and is far from satisfying the asymptotic sum rule Eq. (17); note that the natural mass scale of the dimensionful integral is  $M_\rho^2 \approx 0.6 \text{ GeV}^2$ . The asymptotic sum rule thus requires substantial contributions from energies  $s > s_{\text{max}}$ . An interesting question is whether the pQCD result could account for this missing contribution. Integrating

<sup>2</sup>We use the updated arXiv version of Ref. [36], which matches the recent calculation in Ref. [37] when accounting for scheme- and scale dependencies. We assume an asymptotic distribution amplitude and factorization scale  $\mu = Q$ .

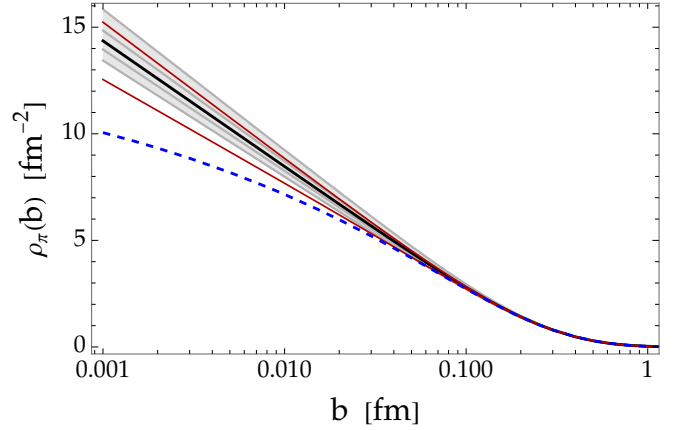


Figure 2: Pion transverse charge density  $\rho_\pi(b)$  computed with the imaginary part of pion FF extracted from the logarithmic dispersion relation (see Fig. 1) and various high-energy completions. *Solid black line*: Density from dispersion integral with finite cutoff  $s_{\text{max}} = (2.5 \text{ GeV})^2$ . *Inner and outer gray bands*: Statistical and total uncertainty from data below  $s_{\text{max}}$ . *Solid red lines*: Density with high-energy completion Eq. (26) with  $\epsilon = 1$  (asymptotic sum rule disregarded). *Dashed blue line*: Same with  $\epsilon = 0.11$  (asymptotic sum rule satisfied).

$\text{Im} F_\pi^Q(s)$  of Eq. (21) from  $s_{\text{max}}$  to infinity we obtain (at LO, NLO, NNLO accuracy)

$$\frac{1}{\pi} \int_{s_{\text{max}}}^{\infty} ds \frac{\text{Im} F_\pi^Q(s)}{s} \Big|_{\text{pQCD}} = -\underbrace{0.0025}_{\text{LO}} - \underbrace{0.0011}_{\text{NLO}} - \underbrace{0.0006}_{\text{NNLO}}, \quad (24)$$

$$\frac{1}{\pi} \int_{s_{\text{max}}}^{\infty} ds \text{Im} F_\pi^Q(s) \Big|_{\text{pQCD}} = -\underbrace{0.114}_{\text{LO}} - \underbrace{0.030}_{\text{NLO}} - \underbrace{0.013}_{\text{NNLO}} \text{ GeV}^2. \quad (25)$$

Adding these contributions to Eqs. (22) and (23) leaves intact the charge sum rule Eq.(16) but is by far not sufficient to fulfill the asymptotic sum rule Eq.(17). Even lowering the lower limit of the integral in Eq. (25) to  $s_{\text{max}} = 1 \text{ GeV}^2$ , the pQCD result can not account for the missing strength (see also Ref. [30]). The origin of the missing strength in the asymptotic sum rule, and indeed the status of the sum rule itself, therefore remain unclear. These circumstances need to be taken into account in the uncertainties of the transverse density.

## 5. Transverse density and uncertainties

We now evaluate the transverse density in the dispersive representation Eq. (3) and estimate its uncertainties. They arise from the uncertainty of the imaginary part in the region  $s < s_{\text{max}}$ , and the possible contributions from  $s > s_{\text{max}}$ .

*Small distances.* Figure 2 shows the extracted density at short distances. The black line gives the density obtained by numerical evaluation of the dispersion integral Eq. (3) with the upper limit  $s_{\text{max}}$ . The inner gray band shows the uncertainty of the density due to the statistical uncertainty of the imaginary part (see Fig. 1). The outer gray band shows the

uncertainty of the density due to the total (statistical and systematic) uncertainty of the imaginary part. The statistical uncertainties were computed by averaging over the MC ensemble, where each instance satisfies analyticity and the logarithmic dispersion relation Eq. (20); the method takes into account correlations in the data and propagates them into the density (a similar procedure was used for nucleon densities in Ref. [25]). One observes: (i) The density exhibits an approximate  $\log(1/b)$  growth at small  $b$ . This is a direct consequence of the nonzero value of the integral Eq. (23), which together with Eq. (18) implies a short-distance behavior as  $\rho_\pi(b) \sim [\text{integral Eq. (23)}] \times \log(1/b)/(2\pi)$ . (ii) The relative uncertainties of the density grow with decreasing  $b$ , as the dispersion integral becomes more sensitive to higher  $s$ , where data have large uncertainties.

To estimate the uncertainty coming from the region  $s > s_{\max}$ , we need to make assumptions about the high-energy behavior of the imaginary part. Naively, one expects that this uncertainty becomes relevant at distances below  $b \sim 1/\sqrt{s_{\max}} = 0.08$  fm. In view of the principal questions regarding the high-energy behavior (onset of pQCD behavior, status of asymptotic sum rule), we content ourselves with simple models realizing different scenarios. These models are used only to estimate the incompleteness error by enforcing the sum rules, not to predict the actual density (see e.g. Refs. [40, 41]).

A minimal model of  $\text{Im} F_\pi^Q(s)$  at  $s > s_{\max}$  is to extend the extracted values at  $s_{\max}$  with a (fractional) power behavior,

$$\text{Im} F_\pi^Q(s) = \text{Im} F_\pi^Q(s_{\max}) \left( \frac{s_{\max}}{s} \right)^{1+\epsilon}, \quad \epsilon > 0. \quad (26)$$

As the first scenario we take  $\epsilon = 1$ , which would be obtained from a vector dominance model of the FF with constant width, disregarding the asymptotic sum rule. Taking the extreme values of the extracted imaginary part at the maximum energy,  $\text{Im} F_\pi^Q(s_{\max}) = \{-0.056, 0.027\}$ , and extending them with Eq. (26), we compute the densities combining the contributions from  $s < s_{\max}$  and  $s > s_{\max}$ . The solid red lines in Fig. 2 show the resulting range. One observes: (i) The high-energy extension has negligible effect at  $b > 0.01$  fm. (ii) The densities obtained with this high-energy extension continue the  $\log(1/b)$  growth at small  $b$  observed in the  $s < s_{\max}$  partial result, which follows from the violation of the sum rule Eq. (17) and cannot prevail down to arbitrarily small distances.

An alternative scenario is to impose the asymptotic sum rule Eq. (17). For this we take Eq. (26) with the central value  $\text{Im} F_\pi^Q(s_{\max}) = -0.03497$  and choose  $\epsilon$  such that the sum rule is satisfied, which gives  $\epsilon = 0.11$ . This describes an imaginary part with a strong power-like high-energy tail of negative sign.<sup>3</sup> The dashed blue line in Fig. 2 shows the density obtained with this high-energy extension. One observes: (i) The small- $b$  behavior of the density is now softer, and the  $\log(1/b)$  growth is absent, in accordance with the findings of Sec. 3.

<sup>3</sup>A similar power-like tail is obtained in the dual resonance model of Ref. [42]. Unfortunately this model cannot be matched directly with the empirical result, because the alternating sign of resonances displayed in Fig. 1 is not reproduced in the model [32].

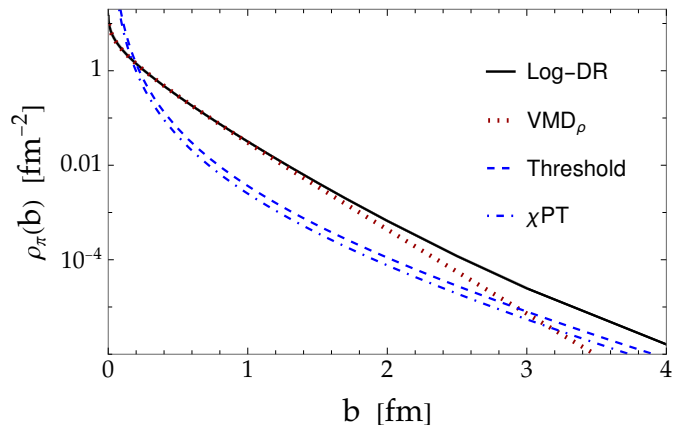


Figure 3: Pion transverse charge density at large distances. *Solid line*: Result of logarithmic dispersion relation (uncertainties not visible on the scale shown here). *Dotted red line*: Density from zero-width  $\rho$  meson pole Eq. (12). *Dashed blue line*: Asymptotic behavior from threshold expansion, Eq. (8). *Dashed-dotted blue line*: Asymptotic behavior from LO chiral perturbation theory, Eq. (10).

With the sum rule now satisfied, Eq. (18) implies a behavior as  $\rho_\pi(b) \sim c + \mathcal{O}[b^{2\epsilon} \log(1/b)]$  for  $\epsilon > 0$ . (ii) The high-energy behavior in this scenario affects the density at distances  $b < 0.1$  fm, in agreement with the naive estimate.

The power-like extension Eq. (26) does not satisfy the QCD asymptotic behavior. One could amend the parametrization to include a pQCD tail above some energy  $s_{\text{pQCD}} > s_{\max}$  and adjust the parameters such that both sum rules are satisfied. The pQCD tail obtained in this way is found to have negligible effect on the density at the distances  $b > 10^{-3}$  fm shown in Fig. 3. In particular, the  $\log \log(1/b\Lambda_{\text{QCD}})$  term in Eq. (19) becomes numerically comparable to the constant term  $c$  only at extremely small distances  $b \lesssim 10^{-10}$  fm. The double logarithmic asymptotics thus plays no role at realistically accessible distances.

In summary, the density is determined by our analysis down to distances  $b \sim 0.1$  fm with controlled uncertainties. Its behavior at smaller distances depends on the assumed high-energy behavior of imaginary part. If the asymptotic sum rule is disregarded, the density is accurately determined by the dispersion relation down to  $b \sim 10^{-3}$  fm, with relative uncertainties reaching  $\sim 20\%$  at the lower end. The  $\log(1/b)$  rise, first observed in the analysis of spacelike FF data [31], continues down to these distances. If the asymptotic sum rule is imposed, and the required negative contributions are assumed to come from energies directly above the measured region, the behavior of the density is qualitatively different. The rise of the density is slowed down; however no indications of  $\log \log(1/b)$  asymptotic behavior can be expected over the range covered here.

*Large distances.* Figure 3 shows the extracted density at large distances on a logarithmic scale (the uncertainties are not visible on this scale). At distances  $b \gtrsim 1/M_\rho$  the contributions from energies  $s > s_{\max}$  are negligible, and the uncertainty of  $\rho_\pi(b)$  arises solely from the statistical and systematic errors of the dispersion integral. One observes: (i) The empirical density agrees very well with the result of the zero-width  $\rho$  meson

pole, Eq. (12), up to  $b \sim 2$  fm. (ii) The asymptotic behavior obtained from the threshold expansion, Eq. (8), approximates the density only at very large distances  $b > 4$  fm, where it is negligibly small. (ii) The LO chiral perturbation theory result Eq. (10) provides a reasonable estimate of the full threshold expansion result Eq. (10).

## 6. Implications for partonic structure

The results for the transverse charge density have interesting implications for the partonic structure of the pion.

*Positivity and attractive  $\pi\pi$  interactions.* In the partonic picture the transverse charge density is given by

$$\rho_\pi(b) = \int dx \{e_u[f_u - f_{\bar{u}}](x, b) + e_d[f_d - f_{\bar{d}}](x, b)\}, \quad (27)$$

where  $\{e_u, e_d\} = \{\frac{2}{3}, -\frac{1}{3}\}$  are the quark charges and  $f_i(x, b)$  ( $i = u, \bar{u}, d, \bar{d}$ ) are the quark/antiquark densities depending on the light-front momentum fraction  $x$  and transverse position  $b$ , obtained as the transverse Fourier transform of the GPDs [9, 10]. The functions are particle number densities (probabilities) and individually positive,  $f_i(x, b) > 0$  [43, 44]. At distances of the order of the typical hadronic size of the pion,  $b \sim R_{\text{had}} \sim 1/M_\rho$ , the density in Eq. (27) is dominated by the  $u$  and  $\bar{d}$  valence quark densities and thus positive,  $\rho_\pi(b) > 0$ . In the dispersive representation the density at these distances can be computed through the elastic unitarity formula in terms of the  $\pi\pi$  phase shift  $\delta_1^1(s)$ , Eq. (11). The positivity of the density then requires that  $0 < \delta_1^1(s) < \pi$ , i.e., that the interactions in the  $\pi\pi$  system be attractive. This represents a statement about the hadronic picture that is obtained from matching with the partonic picture.

*$\rho$  meson exchange and partonic diffusion.* The empirical charge density in the pion is very well described by  $\rho$  meson exchange in the hadronic picture (see Fig. 3). In the partonic picture the transverse distribution arises from the transverse motion of the partons, which involves parton splitting and develops characteristics of a diffusion process [45, 46]. Exploring the partonic dynamics that produces the transverse profile of  $\rho$  meson exchange is an interesting direction for further study, closely connected with the notion of parton-hadron duality.

*Small-size  $q\bar{q}$  configurations in pion.* In the parton picture the pion is described as a quantum-mechanical system in quark/gluon degrees of freedom, containing configurations with varying particle number and spatial size. The transverse charge density represents a probability density of the wave function and thus provides information on the distribution of configurations in the system. The theoretical analysis of Ref. [16] shows that a rising charge density at  $b \ll R_{\text{had}}$  requires the presence of small-size  $q\bar{q}$  configurations in the pion (minimal Fock component, non-exceptional momentum fractions, transverse sizes  $r \ll R_{\text{had}}$ ), and that it cannot be explained by so-called endpoint configurations (multiparticle Fock components, exceptional momentum fractions  $\rightarrow 1$ , transverse size  $r \sim R_{\text{had}}$ ). The large empirical density at  $b \ll 0.1$  fm (in either scenario) implies a substantial probability of small-size  $q\bar{q}$  configurations in the pion [16]. Expressing the scenarios for pQCD asymptotics

and the  $b \rightarrow 0$  limit of the density in the language of partonic configurations presents an interesting problem for further study.

## 7. Conclusions and extensions

The logarithmic dispersion relation for the pion FF allows one to extract the transverse charge density from the cross section of  $e^+e^- \rightarrow \pi^+\pi^-$  exclusive annihilation, a unique case of “transverse imaging” based directly on experimental data. Present data up to  $\sqrt{s_{\text{max}}} = 2.5$  GeV determine the density at  $b \gtrsim 0.1$  fm with controlled uncertainties, including the large-distance behavior where the function is exponentially small. In this region the approach is completely data-driven and offers significant improvements over model-dependent extractions.

The behavior of the density at  $b \lesssim 0.1$  fm depends on qualitative assumptions about the high-energy behavior of  $\text{Im} F_\pi^Q(s)$ . If the asymptotic sum rule is disregarded, the logarithmic dispersion relation determines the density down to much smaller  $b \sim 10^{-3}$  fm, continuing the  $\log(1/b)$  behavior observed around  $b \sim 10^{-1}$  fm. If the sum rule is enforced, the rise of the density is slowed; however, the  $\log \log(1/b)$  dependence in the pQCD asymptotic expression is not visible at any practically relevant distances.

The status of the asymptotic sum rule for the pion FF remains unclear. The empirical  $\text{Im} F_\pi^Q(s)$  shows no sign of satisfying the asymptotic sum rule at energies  $s < s_{\text{max}}$ , even though the charge sum rule is well satisfied. It is unlikely that experiments at slightly higher  $s$  would change the situation. Theory should revisit the principal assumptions in using pQCD approximations in the dispersive approach, or pursue other explanations (e.g. possible heavy resonances).

The present analysis uses the  $n = 1$  logarithmic dispersion relation Eq. (20). It could eventually be extended using the  $n > 1$  relations, which reduce the sensitivity to high energies but involve subtraction constants in the form of the derivatives of the FF or its phase at threshold with high accuracy. The analysis could also be extended to the kaon electromagnetic FF, with a coupled-channel approach accounting for the  $\pi\pi$  cut below the  $K\bar{K}$  threshold.

*Acknowledgments.* CW acknowledges helpful suggestions by Peter Kroll and the late Michael Pennington, and collaboration with Ina Lorenz on an earlier unpublished analysis using logarithmic dispersion relations. ERA acknowledges discussions with Wojciech Broniowski.

This material is based upon work supported by the U.S. Department of Energy, Office of Science, Office of Nuclear Physics under contract DE-AC05-06OR23177. ERA and PSP are partially funded by the Spanish Ministerio de Ciencia Innovación y Universidades (MICIU/AEI/10.13039/501100011033 and ERDF/EU) under grants No. PID2020114767GB.I00 and PID2023.147072NB.I00. PSP is funded by Junta de Andalucía under the grant POSTDOC\_21\_00136 and ERA and PSP under grant FQM225.

## References

- [1] A. V. Radyushkin, Deep Elastic Processes of Composite Particles in Field Theory and Asymptotic Freedom (6 1977). [arXiv:hep-ph/0410276](#).
- [2] G. R. Farrar, D. R. Jackson, The Pion Form-Factor, *Phys. Rev. Lett.* 43 (1979) 246. [doi:10.1103/PhysRevLett.43.246](#).
- [3] A. V. Efremov, A. V. Radyushkin, Asymptotical Behavior of Pion Electromagnetic Form-Factor in QCD, *Theor. Math. Phys.* 42 (1980) 97–110. [doi:10.1007/BF01032111](#).
- [4] G. P. Lepage, S. J. Brodsky, Exclusive Processes in Quantum Chromodynamics: Evolution Equations for Hadronic Wave Functions and the Form-Factors of Mesons, *Phys. Lett. B* 87 (1979) 359–365. [doi:10.1016/0370-2693\(79\)90554-9](#).
- [5] A. V. Efremov, A. V. Radyushkin, Factorization and Asymptotical Behavior of Pion Form-Factor in QCD, *Phys. Lett. B* 94 (1980) 245–250. [doi:10.1016/0370-2693\(80\)90869-2](#).
- [6] G. P. Lepage, S. J. Brodsky, Exclusive Processes in Perturbative Quantum Chromodynamics, *Phys. Rev. D* 22 (1980) 2157. [doi:10.1103/PhysRevD.22.2157](#).
- [7] F. Gross, et al., 50 Years of Quantum Chromodynamics, *Eur. Phys. J. C* 83 (2023) 1125. [arXiv:2212.11107](#), [doi:10.1140/epjc/s10052-023-11949-2](#).
- [8] D. E. Soper, The Parton Model and the Bethe-Salpeter Wave Function, *Phys. Rev. D* 15 (1977) 1141. [doi:10.1103/PhysRevD.15.1141](#).
- [9] M. Burkardt, Impact parameter dependent parton distributions and off forward parton distributions for  $\zeta \rightarrow 0$ , *Phys. Rev. D* 62 (2000) 071503, [Erratum: *Phys.Rev.D* 66, 119903 (2002)]. [arXiv:hep-ph/0005108](#), [doi:10.1103/PhysRevD.62.071503](#).
- [10] M. Burkardt, Impact parameter space interpretation for generalized parton distributions, *Int. J. Mod. Phys. A* 18 (2003) 173–208. [arXiv:hep-ph/0207047](#), [doi:10.1142/S0217751X03012370](#).
- [11] G. A. Miller, Transverse Charge Densities, *Ann. Rev. Nucl. Part. Sci.* 60 (2010) 1–25. [arXiv:1002.0355](#), [doi:10.1146/annurev.nucl.012809.104508](#).
- [12] M. Diehl, Generalized parton distributions, *Phys. Rept.* 388 (2003) 41–277. [arXiv:hep-ph/0307382](#), [doi:10.1016/j.physrep.2003.08.002](#).
- [13] A. V. Belitsky, A. V. Radyushkin, Unraveling hadron structure with generalized parton distributions, *Phys. Rept.* 418 (2005) 1–387. [arXiv:hep-ph/0504030](#), [doi:10.1016/j.physrep.2005.06.002](#).
- [14] S. Boffi, B. Pasquini, Generalized parton distributions and the structure of the nucleon, *Riv. Nuovo Cim.* 30 (9) (2007) 387–448. [arXiv:0711.2625](#), [doi:10.1393/ncr/i2007-10025-7](#).
- [15] V. P. Druzhinin, S. I. Eidelman, S. I. Serednyakov, E. P. Solodov, Hadron Production via  $e^+e^-$  Collisions with Initial State Radiation, *Rev. Mod. Phys.* 83 (2011) 1545. [arXiv:1105.4975](#), [doi:10.1103/RevModPhys.83.1545](#).
- [16] G. A. Miller, M. Strikman, C. Weiss, Pion transverse charge density from timelike form factor data, *Phys. Rev. D* 83 (2011) 013006. [arXiv:1011.1472](#), [doi:10.1103/PhysRevD.83.013006](#).
- [17] C. Bruch, A. Khodjamirian, J. H. Kuhn, Modeling the pion and kaon form factors in the timelike region, *Eur. Phys. J. C* 39 (2005) 41–54. [arXiv:hep-ph/0409080](#), [doi:10.1140/epjc/s2004-02064-3](#).
- [18] T. N. Truong, R. Vinh-Mau, Bounds on the pion electromagnetic form-factor, *Phys. Rev.* 177 (1969) 2494–2500. [doi:10.1103/PhysRev.177.2494](#).
- [19] B. V. Geshkenbein, Pion electromagnetic form factor in the spacelike region and  $P$  phase  $\delta_1^1(s)$  of  $\pi\pi$  scattering from the value of the modulus of the form factor in the timelike region, *Phys. Rev. D* 61 (2000) 033009. [arXiv:hep-ph/9806418](#), [doi:10.1103/PhysRevD.61.033009](#).
- [20] E. Ruiz Arriola, P. Sanchez-Puertas, Phase of the electromagnetic form factor of the pion, *Phys. Rev. D* 110 (5) (2024) 054003. [arXiv:2403.07121](#), [doi:10.1103/PhysRevD.110.054003](#).
- [21] T. P. Leplumey, P. Stoffer, Dispersive analysis of the pion vector form factor without zeros (I 2025). [arXiv:2501.09643](#).
- [22] M. Strikman, C. Weiss, Quantifying the nucleon’s pion cloud with transverse charge densities, *Phys. Rev. C* 82 (2010) 042201. [arXiv:1004.3535](#), [doi:10.1103/PhysRevC.82.042201](#).
- [23] S. Narison, E. de Rafael, On QCD Sum Rules of the Laplace Transform Type and Light Quark Masses, *Phys. Lett. B* 103 (1981) 57–62. [doi:10.1016/0370-2693\(81\)90193-3](#).
- [24] S. Narison, Laplace Sum Rules in Quantum Chromodynamics (9 2023). [arXiv:2309.00258](#).
- [25] J. M. Alarcón, C. Weiss, Transverse charge and current densities in the nucleon from dispersively improved chiral effective field theory, *Phys. Rev. D* 106 (5) (2022) 054005. [arXiv:2204.11863](#), [doi:10.1103/PhysRevD.106.054005](#).
- [26] J. Gasser, H. Leutwyler, Chiral Perturbation Theory to One Loop, *Annals Phys.* 158 (1984) 142. [doi:10.1016/0003-4916\(84\)90242-2](#).
- [27] G. Colangelo, J. Gasser, H. Leutwyler,  $\pi\pi$  scattering, *Nucl. Phys. B* 603 (2001) 125–179. [arXiv:hep-ph/0103088](#), [doi:10.1016/S0550-3213\(01\)00147-X](#).
- [28] R. Garcia-Martin, R. Kaminski, J. R. Pelaez, J. Ruiz de Elvira, F. J. Yndurain, The Pion-pion scattering amplitude. IV: Improved analysis with once subtracted Roy-like equations up to 1100 MeV, *Phys. Rev. D* 83 (2011) 074004. [arXiv:1102.2183](#), [doi:10.1103/PhysRevD.83.074004](#).
- [29] J. F. Donoghue, E. S. Na, Asymptotic limits and structure of the pion form-factor, *Phys. Rev. D* 56 (1997) 7073–7076. [arXiv:hep-ph/9611418](#), [doi:10.1103/PhysRevD.56.7073](#).
- [30] P. Sanchez-Puertas, E. Ruiz Arriola, The electromagnetic pion form factor and its phase, in: 10th International Conference on Quarks and Nuclear Physics, 2024. [arXiv:2410.17804](#).
- [31] G. A. Miller, Singular Charge Density at the Center of the Pion?, *Phys. Rev. C* 79 (2009) 055204. [arXiv:0901.1117](#), [doi:10.1103/PhysRevC.79.055204](#).
- [32] E. Ruiz Arriola, W. Broniowski, Pion electromagnetic form factor, perturbative QCD, and large- $N_c$  Regge models, *Phys. Rev. D* 78 (2008) 034031. [arXiv:0807.3488](#), [doi:10.1103/PhysRevD.78.034031](#).
- [33] B. Ananthanarayan, I. Caprini, I. S. Imsong, Spacelike pion form factor from analytic continuation and the onset of perturbative QCD, *Phys. Rev. D* 85 (2012) 096006. [arXiv:1203.5398](#), [doi:10.1103/PhysRevD.85.096006](#).
- [34] B. Aubert, et al., Precise measurement of the  $e^+e^- \rightarrow \pi^+\pi^-(\gamma)$  cross section with the Initial State Radiation method at BABAR, *Phys. Rev. Lett.* 103 (2009) 231801. [arXiv:0908.3589](#), [doi:10.1103/PhysRevLett.103.231801](#).
- [35] G. J. Gounaris, J. J. Sakurai, Finite width corrections to the vector meson dominance prediction for  $\rho \rightarrow e^+e^-$ , *Phys. Rev. Lett.* 21 (1968) 244–247. [doi:10.1103/PhysRevLett.21.244](#).
- [36] L.-B. Chen, W. Chen, F. Feng, Y. Jia, Next-to-Next-to-Leading-Order QCD Corrections to Pion Electromagnetic Form Factors, *Phys. Rev. Lett.* 132 (20) (2024) 201901. [arXiv:2312.17228](#), [doi:10.1103/PhysRevLett.132.201901](#).
- [37] Y. Ji, B.-X. Shi, J. Wang, Y.-F. Wang, Y.-M. Wang, H.-X. Yu, Next-to-Next-to-Leading-Order QCD Prediction for the Pion Form Factor (11 2024). [arXiv:2411.03658](#).
- [38] T. Gousset, B. Pire, Timelike form-factors at high-energy, *Phys. Rev. D* 51 (1995) 15–24. [arXiv:hep-ph/9403293](#), [doi:10.1103/PhysRevD.51.15](#).
- [39] H.-Y. Chen, H.-Q. Zhou, Two-photon exchange effects in  $e^+e^- \rightarrow \pi^+\pi^-$  and time-like pion electromagnetic form factor, *Phys. Rev. D* 98 (5) (2018) 054003. [arXiv:1806.04844](#), [doi:10.1103/PhysRevD.98.054003](#).
- [40] E. Ruiz Arriola, W. Broniowski, Scalar and tensor meson dominance and gravitational form factors of the pion, in: 10th International Conference on Quarks and Nuclear Physics, 2024. [arXiv:2411.10354](#).
- [41] W. Broniowski, E. Ruiz Arriola, Transverse densities of the energy-momentum tensor and the gravitational form factors the pion, 2024. [arXiv:2412.00848](#).
- [42] C. A. Dominguez, Pion form-factor in large  $N(c)$  QCD, *Phys. Lett. B* 512 (2001) 331–334. [arXiv:hep-ph/0102190](#), [doi:10.1016/S0370-2693\(01\)00576-7](#).
- [43] M. Burkardt, Generalized parton distributions and distribution of partons in the transverse plane, in: Workshop on Lepton Scattering, Hadrons and QCD, 2001, pp. 45–52. [arXiv:hep-ph/0105324](#), [doi:10.1142/9789812799708\\_0006](#).
- [44] M. Diehl, Generalized parton distributions in impact parameter space, *Eur. Phys. J. C* 25 (2002) 223–232, [Erratum: *Eur.Phys.J.C* 31, 277–278 (2003)]. [arXiv:hep-ph/0205208](#), [doi:10.1007/s10052-002-1016-9](#).
- [45] V. N. Gribov, Space-time description of hadron interactions at high-

energies (1973). [arXiv:hep-ph/0006158](https://arxiv.org/abs/hep-ph/0006158).

- [46] A. Capella, U. Sukhatme, C.-I. Tan, J. Tran Thanh Van, Dual parton model, Phys. Rept. 236 (1994) 225–329. [doi:10.1016/0370-1573\(94\)90064-7](https://doi.org/10.1016/0370-1573(94)90064-7).